



Deposited via The University of Leeds.

White Rose Research Online URL for this paper:

<https://eprints.whiterose.ac.uk/id/eprint/155118/>

Version: Accepted Version

---

**Article:**

Alhreez, M, Xiao, X and Wen, D (2019) Kinetic Study of Controlled Asphaltene Inhibitor Release from Nanoemulsions. *Langmuir*, 35 (33). pp. 10795-10807. ISSN: 0743-7463

<https://doi.org/10.1021/acs.langmuir.9b00481>

---

© 2019 American Chemical Society. This is an author produced version of a paper published in *Langmuir*. Uploaded in accordance with the publisher's self-archiving policy.

**Reuse**

Items deposited in White Rose Research Online are protected by copyright, with all rights reserved unless indicated otherwise. They may be downloaded and/or printed for private study, or other acts as permitted by national copyright laws. The publisher or other rights holders may allow further reproduction and re-use of the full text version. This is indicated by the licence information on the White Rose Research Online record for the item.

**Takedown**

If you consider content in White Rose Research Online to be in breach of UK law, please notify us by emailing [eprints@whiterose.ac.uk](mailto:eprints@whiterose.ac.uk) including the URL of the record and the reason for the withdrawal request.

# Kinetic Study of Controlled Asphaltene Inhibitor Release from Nanoemulsions

Mahmoud Alhreez <sup>a</sup>, Xin Xiao <sup>a</sup> and Dongsheng Wen <sup>b, a</sup>

<sup>a</sup> School of Chemical and Process Engineering, University of Leeds, Leeds, UK.

<sup>b</sup> School of Aeronautic Science and Engineering, Beihang University, Beijing, China.

Email address: [d.wen@leeds.ac.uk](mailto:d.wen@leeds.ac.uk) and [d.wen@buaa.edu.cn](mailto:d.wen@buaa.edu.cn)

**ABSTRACT:** The asphaltene aggregation and subsequent precipitation in nonpolar media may have a profound effect on plugging wellbores and production equipment. Continuing our work on controlled release of asphaltene inhibitor by using nanoemulsions (NEs), this work provides new evidence from optical measurement and reveals the release mechanisms kinetically. Multiple light scattering (Turbiscan) and dynamic light scattering (DLS) have been used to study “*in situ*” the effectiveness and performance of controlled release by three cases on asphaltene aggregation/precipitation: i) strong organic acids (dodecyl benzene sulfonic acid, DBSA), ii) nanoemulsions (blank NEs), and iii) nanoemulsions loaded with DBSA (DBSA NEs). The results suggested that the new approach reduced the amount of asphaltene inhibitor by ~ 20 times and achieved high asphaltene inhibition efficiency ~84 % with prolonged release time. A mechanistic understanding of the controlled release effect was proposed based the effect of DBSA NEs on the asphaltene particle morphology variation, which was related to the

hydrophilicity of DBSA and the strong intermolecular interactions among all DBSA NE's components. The release mechanism of the asphaltene inhibitor from the NE was compared with eight release models, and was found to follow the Korsmeyer-Peppas kinetic model.

**KEYWORDS:** Controlled release; release kinetic; asphaltene inhibitor, nanoemulsions, asphaltene precipitation and stability.

## **1- Introduction**

Asphaltenes are macromolecules containing aromatic and naphthenic cores, aliphatic chains, and heteroatoms such as oxygen, nitrogen, or sulfur [1]. Even in low concentrations, asphaltene molecule is prone to aggregate and precipitate, causing plugging of pipelines and process equipment such as pumps, heat exchangers, or separator tanks [2-7]. Chemical treatment using asphaltene inhibitors (AI) is considered as one of the most common strategies to prevent asphaltene precipitation [8,9]. However, it has a major problem due to the loss a large amount of chemicals, resulting in high treatment cost [10]. Using high concentrations of inhibitor tends to produce self-associations in the bulk rather than adsorption on asphaltene, reducing their effectiveness [11,12]. More recently, a considerable work has grown up around the use of oil/water nanoemulsions (NEs) in breaking down asphaltene emulsions [13, 14, 15]. However, efficient methods of enhancing long-term asphaltene stability with reduced AI amount are still much demanded.

Instead of releasing drugs inside a body, NEs are used to release chemicals (i.e. surfactant or polymer) inside a nonpolar media in the oil and gas reservoir either for enhance flow assurance or environmental remediation. In the previous study [16], we developed a novel concept for controlled delivery and release of AI by using NE to control asphaltene precipitation under dynamic force (i.e., centrifugal force). LUMiSizer was utilised to study the effectiveness and

performance of controlled release by three cases on asphaltene sedimentation. It showed that the new concept could provide tremendous value by i) improving the stability of the asphaltene, ii) reducing the usage of AI, and iii) extending the treatment time. In one example study, the optimum inhibitor concentration for completely stabilizing asphaltene can be reduced by ~20 times by using NEs. The total chemical amount was reduced by 10% even by considering all chemicals used in producing NEs. In addition, the release time was greatly extended and a significant delay of asphaltene precipitation, i.e., a delay from pure asphaltene solution of 450 s to 1400 s, was observed in the presence NE. By promoting slower release and provide long-term stability with reduced chemical usage, this novel concept could have obvious implication on asphaltene inhibition. The experiment showed that the release of AI from NE depends on the interactions of surfactants used for the fabrication of NEs, and the subsequent change of the overall polarity and hydrophobic characteristics. However, the release kinetics and mechanism are still unclear.

While controlled delivery techniques are increasingly used for a range of industries such as fragrances in personal care products, insecticides in agrochemicals, nutraceuticals in foods, and drugs in pharmaceuticals, there remain significant limitations for both the characteristic and the kinetic release profile that can be achieved [17]. In most of drug release cases, theoretical fundament does not exist, and empirical equations are generally used [18]. The use of mathematical modelling turns out to be very useful as this approach enables, in the best case, the prediction of release kinetics [19].

In this paper, we conducted a detailed release kinetic study by employing optical technique to monitor the release profile. Three case studies were performed on the stability of asphaltenes: i) strong organic acids (dodecyl benzene sulfonic acid, DBSA), ii) nanoemulsions (blank NEs), and

iii) nanoemulsions loaded with DBSA (DBSA NEs). Those important physical parameters, such as the AI release rate and time, were obtained. Not only providing new evidence to support our previous concept, the data are proceeded and compared with eight established mathematical models, to elucidate the release mechanism.

## **2. EXPERIMENT AND METHODS**

### **2.1. Materials**

Analytical grad materials including crude oil, xylene ( $> 98.5\%$ ), n- heptane (extra pure  $\geq 98\%$ ), Toluene (extra pure  $\geq 98\%$ ), dodecyl benzene sulfonic acid (DBSA), Tween 80 (sorbitan monooleate), and sodium benzene sulfonic acid (SDS) were purchased from Sigma-Aldrich company.

### **2.2. Methods and measurement**

#### **2.2.1. Synthesis of nanoemulsions**

The successful long-term stability of AI inside NEs requires different materials than currently used (surfactants) to create impermeable barriers that can arrest the diffusion of AI from the nanodroplet core. As an example study, DBSA is used in this work to provide steric and electrostatic repulsion together with hydrophobic and acid- base interactions between its molecules and ionic/non-ionic surfactants (i.e., synergistic effect). The procedure of synthesis of NEs with the presence and absence of AI was elaborated in the previous study [16], as depicted in the schematic diagram in Figure 1. Table 1 shows the composition and concentrations of all three cases used in this work.

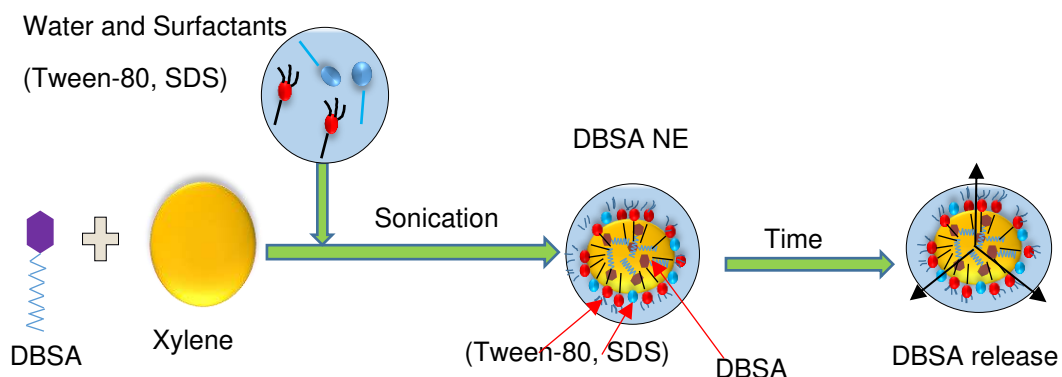


Figure 1: Schematic diagram of synthesis procedure of DBSA NE and the release kinetic during long time.

Table 1: The composition and percentage of all three cases used in this work.

Sample	DBSA (vol.%)	xylene (vol.%)	Tween 80 (vol.%)	SDS (vol.%)	Water (vol.%)
DBSA	4.0	-----	-----	-----	-----
Blank NE	-----	7	9.9	0.1	83
BDSA NE	1.0	7	9.9	0.1	82

### 2.2.2. Asphaltene extraction and preparation of solution.

The separation of asphaltenes was carried out according to ASTM D2007 by mixing crude oil with n-heptane at a volume ratio of 1:40, which is known to destabilize asphaltenes and to give rise in asphaltene precipitation. The procedure of asphaltene extraction was reported previously [16]. For preparation of asphaltene solution, a (0.025 w/v %) of the asphaltene was prepared in a mixture of two solvents: Toluene / heptane (Heptol) volume ratio of 60:40. To examine the effect

of DBSA, blank NEs, and DBSA NEs on asphaltene precipitation, samples were slowly added to asphaltene solutions under shear action in a (IKA T2S digital/Ultra-Turrax) homogenizer at a rotation speed of 8000 rpm until complete incorporation of the NEs into the asphaltene solution.

### **2.3. Characterization**

The determination of asphaltene molecular structure was carried out using X-ray diffractometer (XRD Bruker D8). The XRD patterns of asphaltene samples consists of four major peaks or bands, namely;  $\gamma$  -band, graphene (or 002) band, (10) band, and (11) band. These bands for a typical XRD pattern of asphaltene sample extracted from Iraqi crude oil are illustrated in Figure 2. The  $\gamma$ - band reflects the spacing between aliphatic layers (aliphatic chains or saturated rings) that occurs from the X-rays scattered by the condensed naphthenic rings or the aliphatic chains, which appears around  $2\theta = 20^\circ$ , while the graphene band reflects the spacing between the aromatic layers, which appears around  $2\theta = 20^\circ$ . The (10) and (11) bands reflections come from the inplan structure of aromatics, which reveal the average diameter of the aromatic sheets. The (11) band is generally very weak and often not seen for its very low intensity compared to the (10) band and, therefore, the (10) band at around  $2\theta = 40^\circ$  is normally adopted in the calculation [20]. These findings reflect those of Yen et al. [21] and AlHumaidan et al. [22].

TEM (FEI Titan Themis Cubed 300 TEM) was employed to the influence of DBSA NEs on the asphaltene particles sizes and the morphology of these particles after the adsorption and slowly release. Prior to TEM analysis, samples were dispersed on a TEM grid (holey carbon film, 400 Cu Mesh from Agar Scientific).

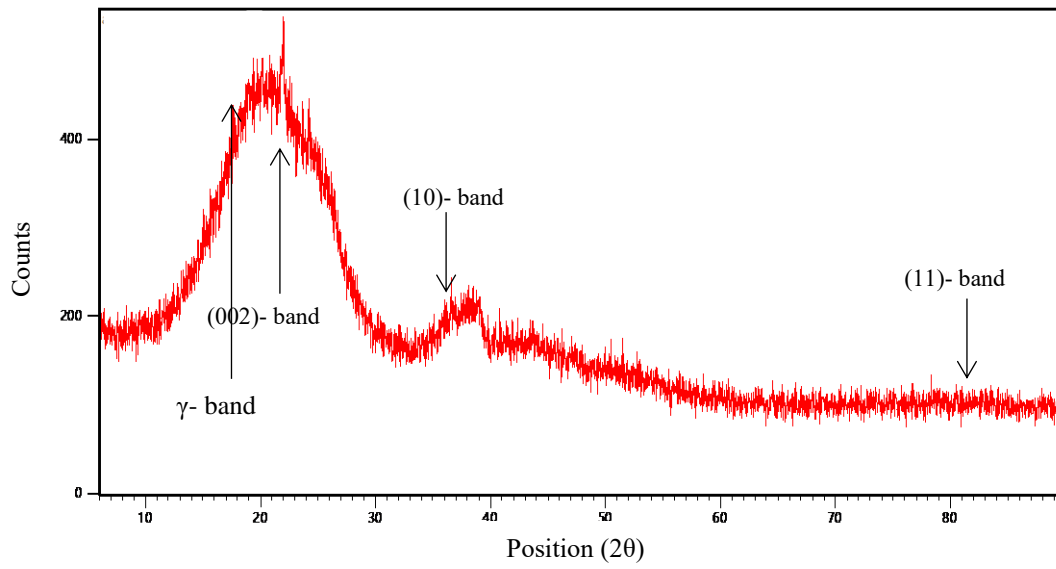


Figure 2: XRD pattern of asphaltene.

#### 2.4. The stability of asphaltene using multiple light scattering

The static stability of asphaltene was evaluated *In-situ* by a Turbiscan instrument (Formulation, France). The sample in the cell was at level (40 mm), and two types of measurements were carried out: i) whole sample scanning continuously for 15 hours where the change in transmissions with position of sample were recorded, and ii) fixed position scanning where the transmissions as a function of time were measured at 25 mm from the top of the sample. Unstable asphaltene forms large particles that precipitate quickly, while stable asphaltene tends to form small aggregates that show small changes in the transmittance profile. Moreover, stability was also assessed by means of the separability number (SN), which is defined as the standard deviation of the average transmittance. A value lower than 5 indicates high asphaltene stability, and greater than 10 suggests that the asphaltene is unstable, whereas a value between 5 and 10 means medium stability [23, 24]. The transmission of asphaltene sample and treated samples were recorded as (%T<sub>asph.</sub>) and (%T<sub>treated</sub>) respectively. The asphaltene sample was

shaken again on the vortexer such that all the asphaltenes were dispersed in the solution and the transmission was recorded as 100% dispersion (100% *Asph. dispersion*). The percent inhibition (A.I %) was calculated from transmission measurements as per the equation [25]:

$$A.I (\%) = 100 - \left[ \frac{\%T_{treated} - \%Asph.dispersion}{\%T_{Asph.} - \%Asph.dispersion} \right] \times 100 \quad (1)$$

## 2.5. Asphaltene inhibitor release study

Membrane diffusion (i.e. dialysis) method is considered as one of the most convenient techniques for determining the drug release profiles of nano-sized drug delivery systems like nanoparticles, liposomes, nanosuspensions, emulsions [26-28]. With the same mechanism and methodology, the dialysis bag (12 kDa) was filled with known amount of DBSA NEs, which was immersed into 300 ml of Heptol/ethanol mixture (7:3 in volume) (i.e., acceptor) [28]. Similarly, DBSA dissolved directly in xylene was also filled into the dialysis bag. Four DBSA concentrations in both cases were used: 1.0 vol. %, 2.0 vol. %, 3.0 vol. % and 4.0 vol. %. The release and transport of DBSA from the dialysis bag into the acceptor medium could be accelerated using a magnetic stirrer and was set to 400 rpm to assure constant agitation of the acceptor compartment. A total of 1 ml of sample was collected at predetermined time interval and equal volume of acceptor medium was replaced. DBSA was quantified using UV-visible spectrophotometry, at the wavelength of 320 nm, based on previously prepared calibration curve using the following equation:

$$DBSA \text{ released } (\%) = \frac{DBSA \text{ in respecter media}}{\text{Total DBSA added}} \times 100 \quad (2)$$

The existing experimental method for measuring AI release kinetics is shown in Figure 3.

Once the profiles of released and transport DBSA through the membrane from NEs and xylene were obtained, different models could be used to fit the results in order to study the kinetics of DBSA released through membrane between 0 and 24 h. The release kinetics was determined by linear regression analysis of the release curves in eight models: zero order (cumulative amount (%) of inhibitor released with time), first order (log cumulative amount (%) of inhibitor released with time), Higuchi (cumulative amount (%) of inhibitor released with the square root of time), Korsmeyer-Peppas (log cumulative amount (%) of inhibitor released with log time), Hixon–Crowell, square root of mass, three seconds root of mass and Baker–Lonsdale models [18,29], as summarized in Table 4. The best-fit kinetics model was selected based on the based on the highest coefficient of determination ( $R^2$ ).

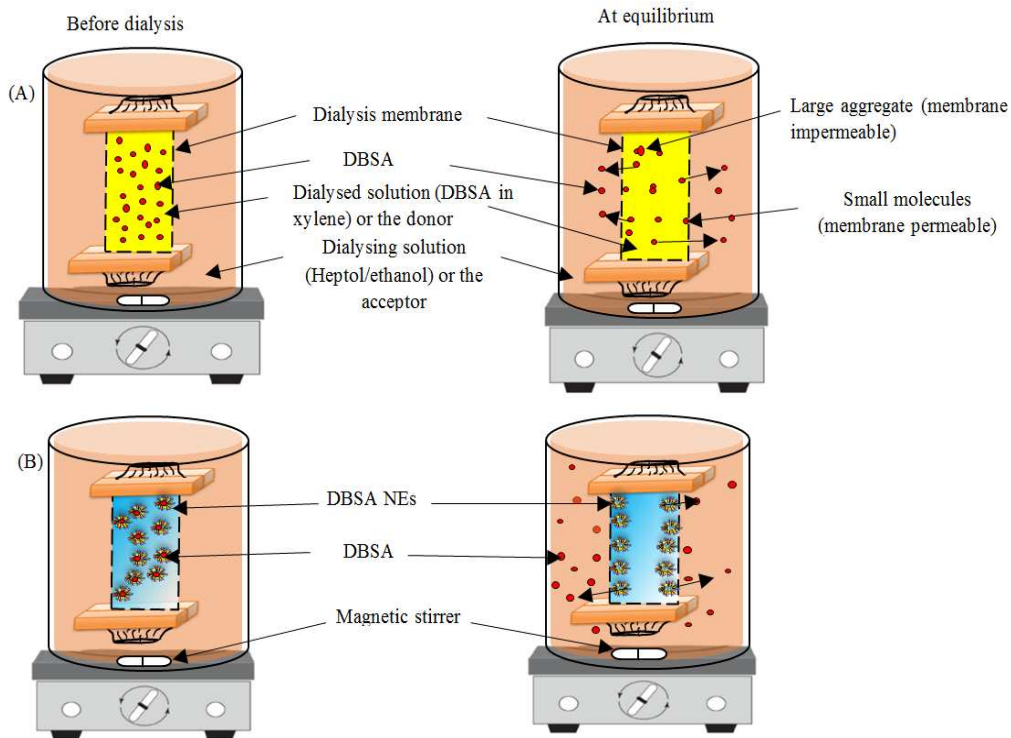


Figure 3: Schematic of the inhibitor release through a dialysis membrane. A) Direct loading method (DBSA in xylene) and B) DBSA NEs. Inhibitor releases through the dialysis membrane into the outer compartment holding release medium.

## **2.6. Methodology applied in the construction of transmission % – cumulative inhibitor released % (point-to-point relationship)**

In order to validate the best-fit kinetics release model to stabilise asphaltene, the membrane dialysis method data (% cumulative of DBSA released versus time) was retrieved from studies described in Section 2.5, and the Turbiscan technique data (% transmission versus time) was obtained from a study described in Section 2.4. This relationship was generated by plotting the % cumulative of DBSA released on the X-axis and the corresponding % transmission on the Y-axis at same time points. The model (linear or polynomial) with the best regression coefficient was selected and used for validation.

## **3. Results and discussion**

### **3.1. The stability of asphaltene using optical techniques**

An analytical stability of asphaltene technique, the Turbiscan, has been recently used as “*in situ*” tool to characterize the stability of colloidal dispersions for early formulation stability within shorter and longer timescales [30-32]. However, this technique has received little attention in the field of asphaltene sedimentation or precipitation. The multiple light scattering method is adopted in this work to examine the effect of controlled release by investigating the stability of asphaltene particles by three case studies with: i) DBSA, ii) blank NE, and iii) DBSA NE, as below:

The results demonstrate that when the asphaltene is destabilized by the addition of n-heptane (0.025 w/v % asphaltene in 60:40 volume ratio Heptol), the transmission of asphaltene showed an increase with time, resulting in a quick formation of aggregation into larger structures, settling

down faster. However, after the addition of 4 vol. % DBSA to the asphaltene solution, the asphaltene particles are sterically stabilized by the presence of DBSA molecules on the asphaltene particle. Under this condition, the individual particles are kept into the asphaltene sample without any aggregation or sedimentation. In addition, no significantly change in transmission for asphaltene solution was observed after 24 h under gravity force, as shown in Figures 4b and 5. This can be attributed to the effectiveness of DBSA to interact with asphaltene molecules, which is kept the asphaltenes well-solubilized in the solution; as a result, the transmission remains unchanged within 24 h.

The transmission data for asphaltene particles with blank NEs is considered in Figures 4c and 5. It is obvious that the transmission is seen to progress in a linear fashion with time. For asphaltene with 20 vol. % blank NE sample, the transmission decreases compared with the transmission for asphaltene solution over extended times; therefore, these findings suggest that the NEs have a moderate influence on asphaltene stabilization comparing with using 4 vol. % DBSA. The stability behaviour can be attributed to the presence of components of blank NEs such as water, surfactants, and xylene that interact with asphaltene molecules.

In the case of the addition of DBSA NEs, the transmission slightly increases after 2 h due to settle down of large asphaltene particles and then gradually decreases within extended time, which indicates that the release effect plays a significant role in the process. It may be assumed that, in this case, the DBSA and other NE's components were progressively released from NE and interact with asphaltene molecules, which is saturated the H-bonding sites of asphaltenes and the fact that it interacted with both the periphery and aromatic cores of asphaltenes, suggesting that the asphaltene is prevented from interacting laterally between themselves and kept well-solubilized in the solution i.e., increasing the stability of asphaltene. These interactions are

almost certainly due to acid-base interaction, hydrogen bond, polar- $\pi$  interaction, cation- $\pi$  interaction and aromatic – aromatic interaction. These interactions can also promote further electrostatic interactions with other ion pairs. For example, the hydroxyl group in the chain length can form H-bonding with water or surfactants, whereas the nitrogen in the aromatic core can provide acid–base as well as H-bonding interactions with DBSA. Therefore, using a small amount of DBSA (1 vol. %) with other components in the DBSA NEs is sufficient to produce a complete coverage of the individual aggregates. Figure S1 in the Supplementary Information shows a schematic attachment of DBSA NE components with asphaltene.

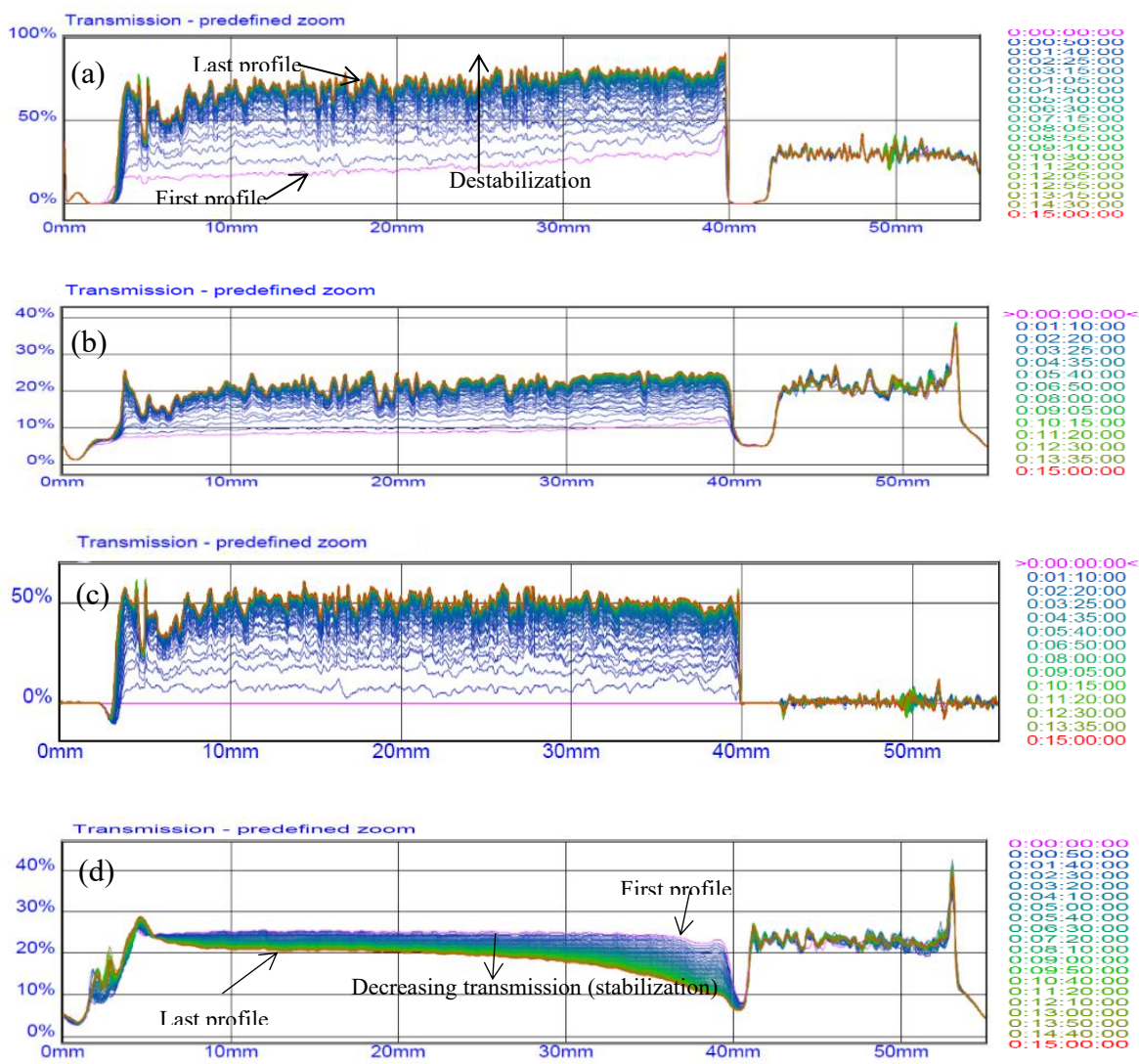


Figure 4: Transmission profiles for (a) asphaltene, (b) 4 vol. % DBSA, (c) 20 vol. % blank NE, and 20 vol.% DBSA NE during 15 h of continuous test at 25 °C.

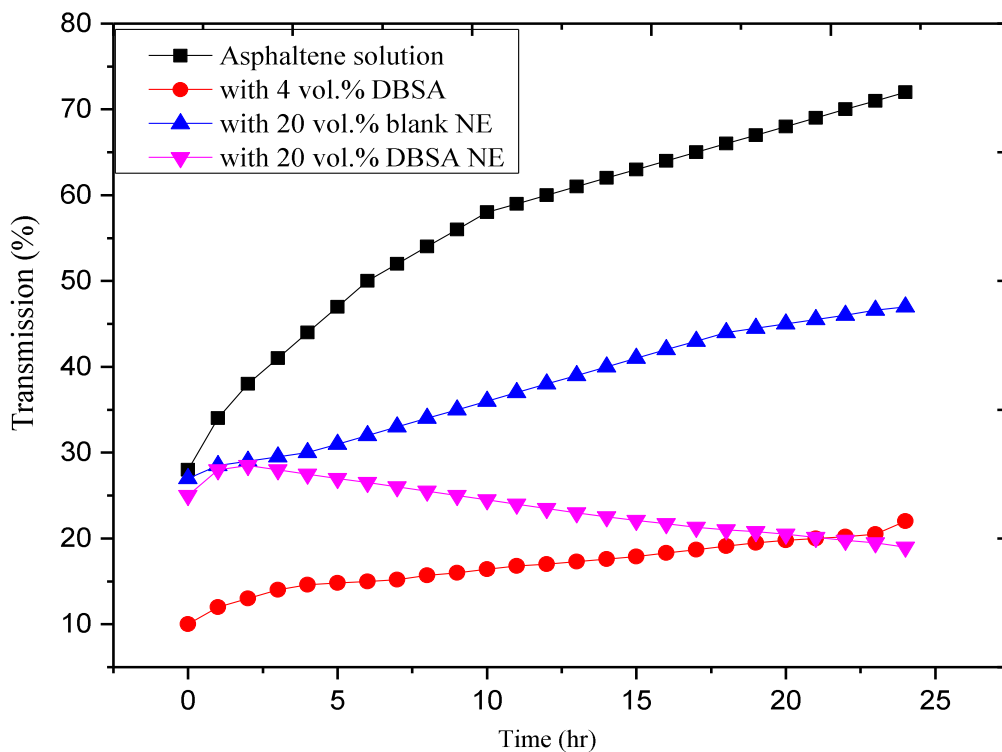


Figure 5: Transmission profiles at fixed position (25 mm) for asphaltene, 4 vol. % DBSA, 20 vol. % blank NE and 20 vol. % DBSA NE during 24 h of continuous test.

The effect of these three cases on the stability of asphaltene is further examined by determining the separability number (SN) (%). Interestingly, the asphaltene with 4 vol. % DBSA reduces SN from 12.18 (for asphaltene solution) to 2.76, indicating that asphaltene stability is increased. However, asphaltene with blank NEs reduces SN to 7.22. It can thus be suggested that the addition of blank NEs to asphaltene solution categorizes them as "moderately stable" when the separability number is between 5 and 10.

Coming back to the topic of the role of DBSA NEs in asphaltene stability, these experiments have shown that there is a significant effect of the DBSA NEs on asphaltene stability by reducing

SN from 12.18 to 2.9. Therefore, the results of stability as found by separability number are more superior, accurate and highly sensitive.

The percent of asphaltene inhibition (A.I %) was also calculated from each transmission by using Eq. (1) to evaluate the performance of three cases on asphaltene stability. These findings for average transmission, A.I %, and SN data provide further comparison between the three cases, which show that asphaltenes treated by 20 vol. % DBSA NE has similar effect as that of 4 vol. % DBSA. However, the treatment by 20 vol. % blank NE still has some effect but less strong the other two. To illustrate the effect of inhibitor (i.e. DBSA) reduction, the transmission, A.I %, and SN are plotted in Figure 6. Using 20 vol.% DBSA NEs (i.e., containing 0.04ml DBSA) give nearly the same values of average transmission, SN, and A.I % as that of 4 vol.% DBSA (i.e., about 0.8 ml). Therefore, the amount of AI (%  $R_{AI}$ ) is decreased by 95%. Although DBSA NEs contain different chemicals such as xylene, surfactants, and DBSA, the total chemicals (%  $R_{TC}$ ) are again lower than 4 vol.% DBSA by a factor of 10%, as shown in clearly in the detailed materials balance are shown in Tables S1 in the Supplementary Information. These results in good agreement with the previous work [16] for reducing AI amount and the total chemicals used, which found that 4 vol. % DBSA and 20 vol. % of DBSA NEs gave the same values of instability index and sedimentation rate.

Furthermore, the results of the efficiency of asphaltene inhibition provide compelling evidence for long-term stability with high efficacy and suggest that this approach appears to be effective with increasing release time. From the data in Figure 7, it is apparent that, for asphaltene with DBSA NEs after 24 h of aging, the A.I % increases with time (i.e. increasing from 15 to 84.12 % gradually) due to the release effect, while for asphaltene with 4 vol. % DBSA the A.I % decreases with time (i.e. decreasing from 89 % to 79.3 %). Consequently, it can be suggested

that the DBSA NEs provide cost-effective and long-lasting stability, and this is invaluable method to control asphaltene precipitation.

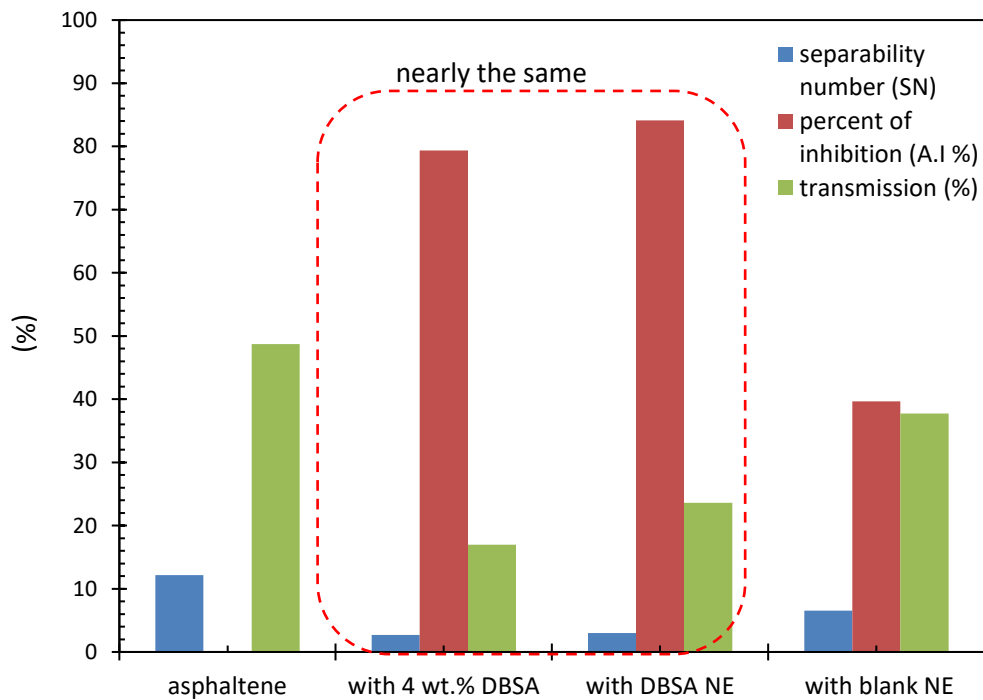


Figure 6: Separability number and average transmission for asphaltene, 4 vol. % DBSA, 20 vol.% blank NE, and 20 vol.% DBSA NE.

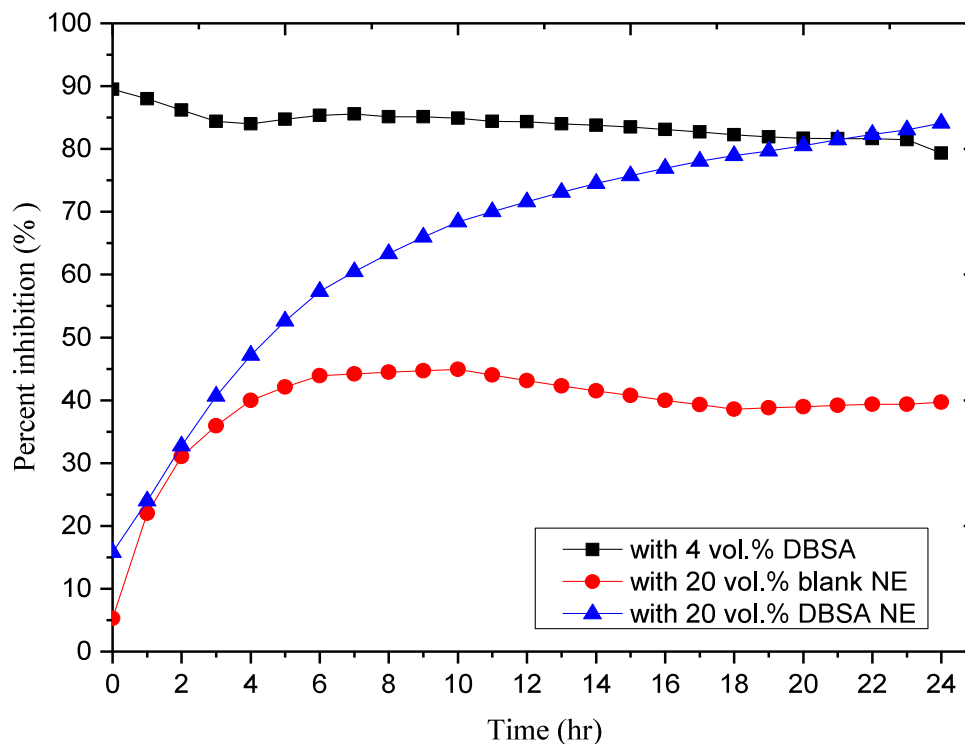


Figure 7: The percent of inhibition (A.I %) for asphaltene with 4 vol. % DBSA, blank NEs, and DBSA NEs with time.

### 3.2. The effect of DBSA NEs on the size and morphology of asphaltene

To validate the effect of DBSA NEs on the sizes of asphaltene precipitates, samples were collected from both the bulk and the bottom of sample (i.e. sediment bed) for asphaltene in the presence and absence of DBSA NEs after 24 h of aging time in order to measure particle sizes using DLS. We found that the asphaltene bulk contains fine particles of 5 – 20 nm, suggests that all larger particles in the bulk are precipitated down towards the bottom of sample. Whilst the sediment bed showed formation asphaltene precipitates into larger structures within the ranges of 1000 –3073 nm. On the other hand, asphaltene solution with DBSA NEs is found containing small particles of 10 - 60 nm in the bulk, suggests that DBSA NEs make the bulk more size polydisperse than asphaltene without DBSA NEs. Moreover, the sample taken from sediment

bed shows no significantly change in asphaltene particle sizes, this may due to the stability of sample without sedimentation or precipitation. It can be seen in Figure 8 (a and b) that the size distribution of the asphaltenes particles in both bulk and sediment bed were narrower compared with asphaltene without DBSA NEs, that also is evidence to indicate that the DBSA NEs are able to reduce asphaltene particles from precipitate and form a good dispersion in the medium. The data presented in Figure 8 b also confirmed that using 4 vol. % DBSA and 20 vol. % of DBSA NEs gave nearly the same values of particle sizes and size distribution of the asphaltenes in both bulk and sediment bed. These findings are broadly consistent with the data collected using the Turbiscan and with those obtained by Mansur et al. [33]. Table 2 shows the particle sizes and polydispersity index data of both supernatant and sedimentation bed for asphaltene with and without 4 vol. % DBSA and 20 vol. % DBSA NEs after 24 h.

The release mechanism is supported by the evidence of the transmission electron microscopy that the DBSA NEs were firstly added to the dispersion of asphaltenes under shear action in a homogenizer until complete incorporation of the DBSA NEs into the oil phase. The water phase which contains nanodroplets forms a layer around the asphaltene particles [23, 24]. Nanodroplets adsorb on asphaltene particles due to its high lipophilicity and higher affinity to the asphaltene. Eventually, the DBSA inside NEs can be slowly released to interact with asphaltene clusters, and hence the larger asphaltene particles are reduced and kept well-stabilized in the bulk. Figure 9 shows the optical and transmission electron microscopy at different steps of asphaltene stability via slowly release of DBSA from NEs.

Although the proposed mechanism is well presented and evaluated by the effect of DBSA NEs on the asphaltene particle size, more validation about its effect on the morphology is still demanded. Figure 9 c presents the micrographs of asphaltenes in 60:40 Heptol solution with and

without DBSA NE after 24 h of releasing test. Without DBSA NE, large asphaltene clusters interacted with each other and grew into asphaltene precipitates to form rodlike shape structures. However, DBSA NEs are able to reduce asphaltenes from precipitate to spherical nanometric particles having a diameter of around 5 to 30 nm with a large stacking distance ( $d_m$ ) between aromatic rings of asphaltene about 0.389 nm. It is evident that these results are in good agreement with those obtained by DLS. A possible explanation for this might due to very strong intermolecular interactions, which provide a complete coverage of the individual aggregates to interact with both all periphery and aromatic cores of asphaltenes. This explained why DBSA NEs favored the formation of nanoaggregates with spherical rather than rodlike shape structures. However, the formation of rodlike shape structures is might be contributed to the onset of asphaltene precipitation is near 60:40 Heptol, in excellent agreement with recent studies [33 35]. These rodlike shape structures have an average size of 500 nm, while the spherical particles equivalent size of these structures is approximately 10 nm in the same volume ratio of Heptol. This indicates that DBSA NEs are able to delay the precipitation onset in 60:40 toluene/heptane solutions.

Table 2: Particle sizes and polydispersity index data of both supernatant and sedimentation bed for pure asphaltene and asphaltene with 4 vol. % DBSA and DBSA NEs after 24 h.

Sample	Size (nm)	PdI
Asphaltene (bulk)	5.577	0.570
Asphaltene (sediment bed)	3019	0.350
Asphaltene with 4 vol. % DBSA (bulk)	28	0.200
Asphaltene with 4 vol. % DBSA (sediment bed)	95	0.293
Asphaltene with DBSA NE (bulk)	19	0.120
Asphaltene with DBSA NE (sediment bed)	58.44	0.223

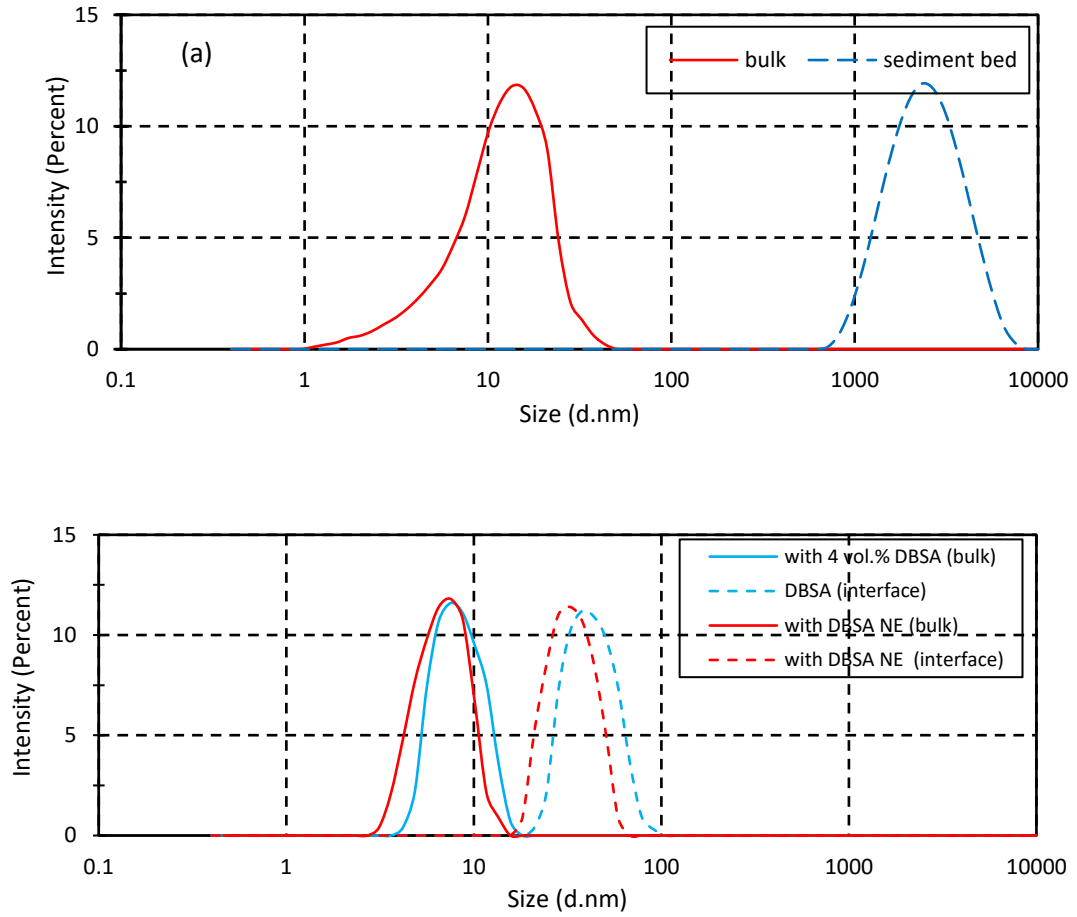


Figure 8: Size distribution data of both bulk and sedimentation bed or interface for (a) asphaltene, and (b) asphaltene with DBSA NEs and 4 vol. % DBSA.

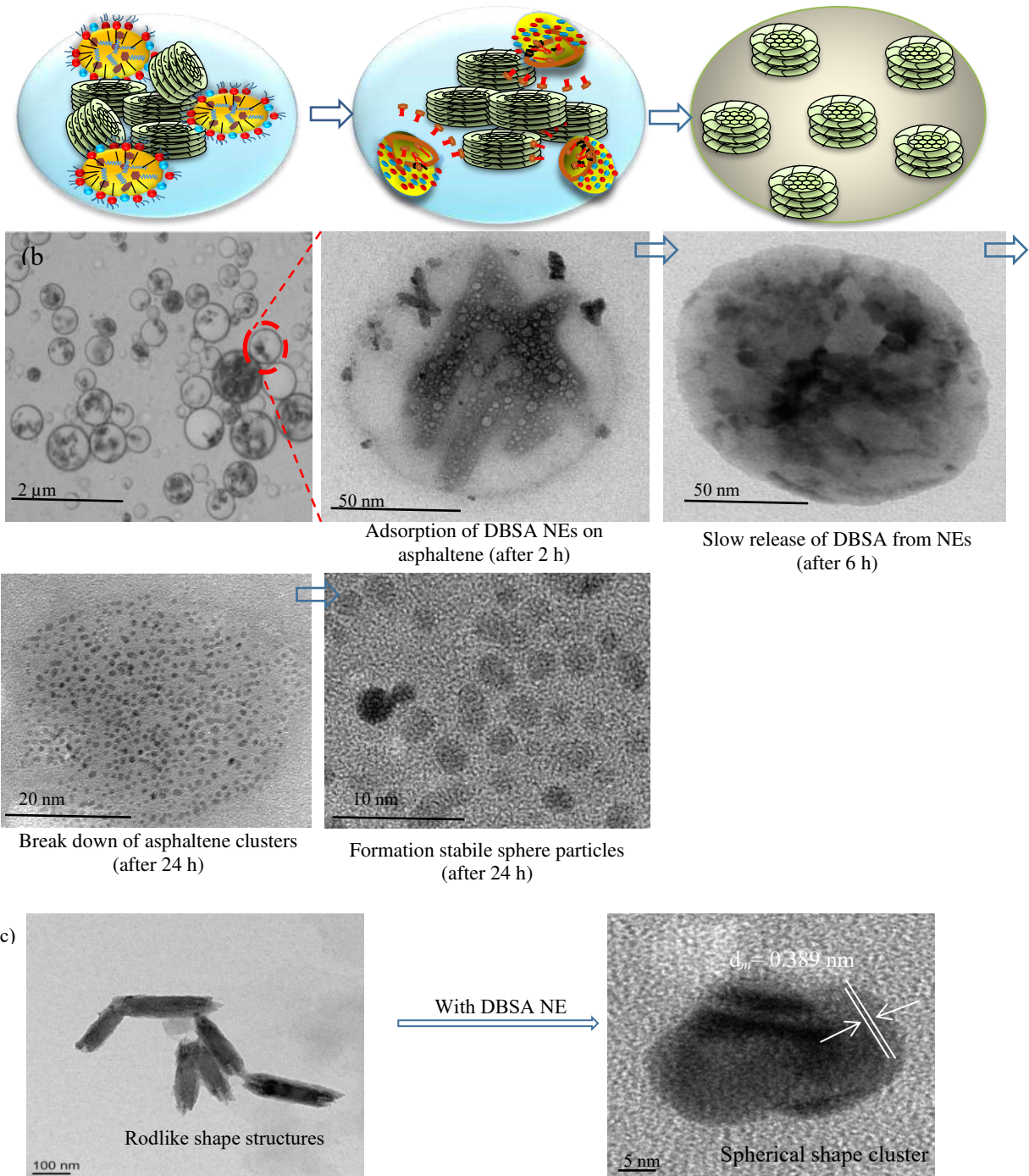
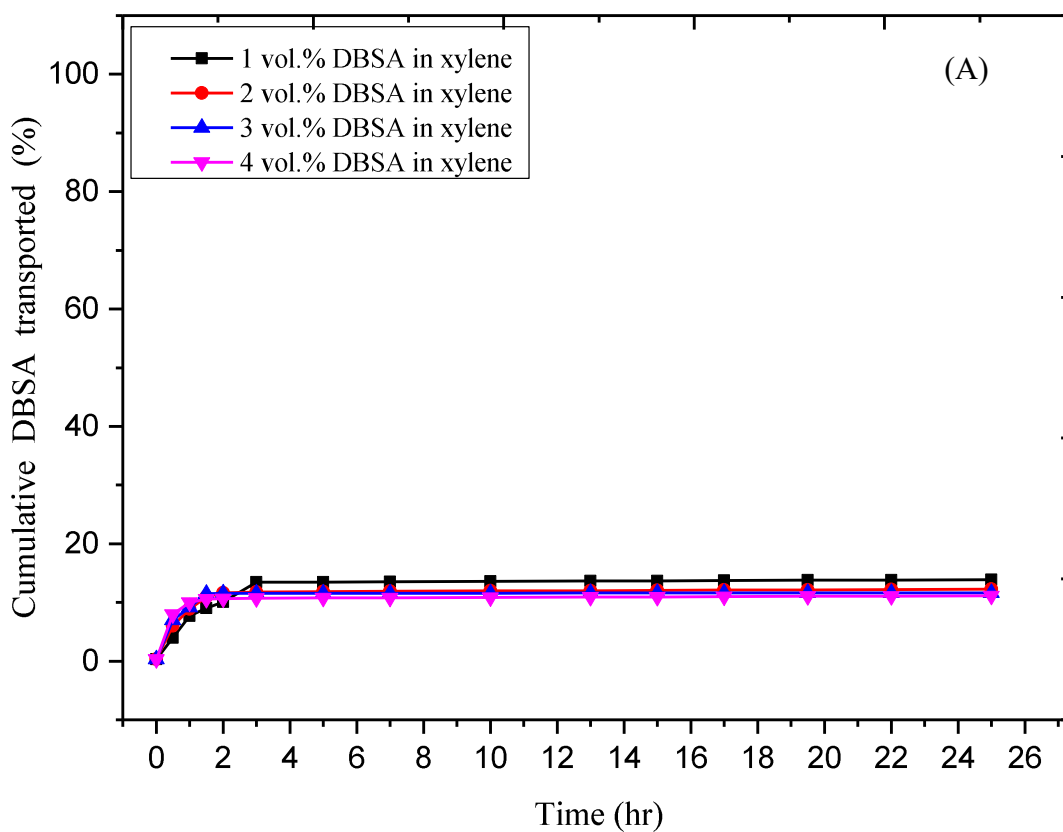


Figure 9: (a) Schematic diagrams of different steps of asphaltene stability via slow release DBSA from NEs; (b) optical and electron microscopy images of the asphaltene with DBSA NEs. The micrographs correspond to different times and are chosen to illustrate the release effect; (c) the effect DBSA NEs on the shape and size particles.

### **3.3. Kinetic study of inhibitor release through the dialysis membrane**

The kinetic processes of inhibitor transport and release through the dialysis membrane are examined for two cases: NEs loaded DBSA and DBSA directly dissolved in xylene. This procedure is similar to drug release in the area of nanomedicine by using the dialysis bag method [26-28] (see Section 2.4). The rate of DBSA released through the dialysis membrane was measured for both cases at different DBSA concentrations: 1 vol. %, 2 vol. %, 3 vol. %, and 4 vol. %, as shown in Figure 10. At low concentration (1 vol. %), it is noticed that the transport of DBSA from xylene shows initial burst behaviour during the first three hours followed by a steady transport through membrane for the following 22 hours, which means that the inhibitor transport is not completely controlled. Initial burst behaviour kinetics and uncontrolled transport through membrane are very common in the use of drug directly with oil [26,27,36]. This behaviour could cause aggregation near the wellbore, leading to a large amount of chemicals loss inside reservoir, resulting in high treatment cost. The data presented in Figure 10b confirmed that the beneficial effect of NEs for controlled DBSA release as compared to the burst and uncontrolled DBSA transport from xylene. It is clear that DBSA NEs demonstrated lower DBSA release at initial time points in comparison with DBSA in xylene, ascribable to the use of mixed surfactants, which offers a physical barrier to inhibitor release from NEs and efficiently control its release. Moreover, the slower release rate from DBSA NEs with mixed surfactants could be attributed to small size of DBSA NEs (i.e., 21 nm), which can provide a high surface area of the system. In fact, higher surface area means more surfaces from which the inhibitor can be released. Therefore, the relatively small burst release and higher sustained release rate of DBSA from NEs can be achieved. However, our results also suggest that the cumulative release or transport of DBSA clearly depend on the amount of inhibitor. The release profiles of DBSA from

NEs tend to decrease as the DBSA concentration increased. This may have been due to droplet growth with increasing the concentration of DBSA inside NEs, which means appreciable amount of DBSA is not released from the droplets into the acceptor media. Similarly, the transport profiles of DBSA molecules from xylene decrease as the DBSA concentration increased in xylene. The drop in the transport profiles of DBSA with increasing the inhibitor concentration may have been due to the formation of large molecules in the donor compartment. Table 3 shows the influence of DBSA concentration and droplet size on the total amount of DBSA released or transported for both cases.



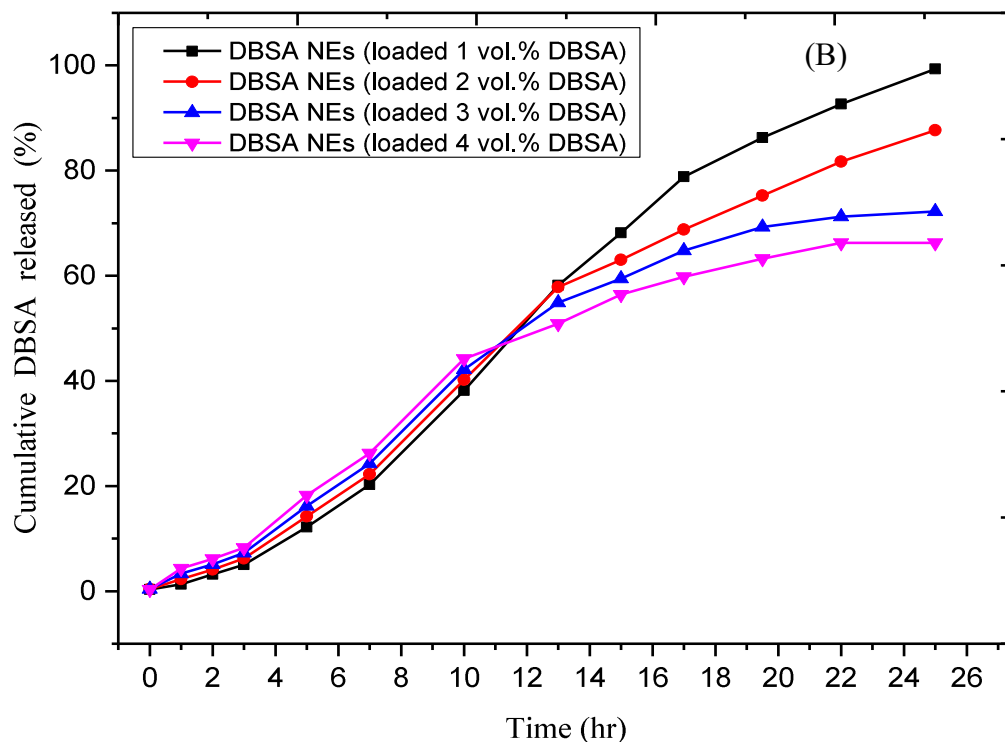
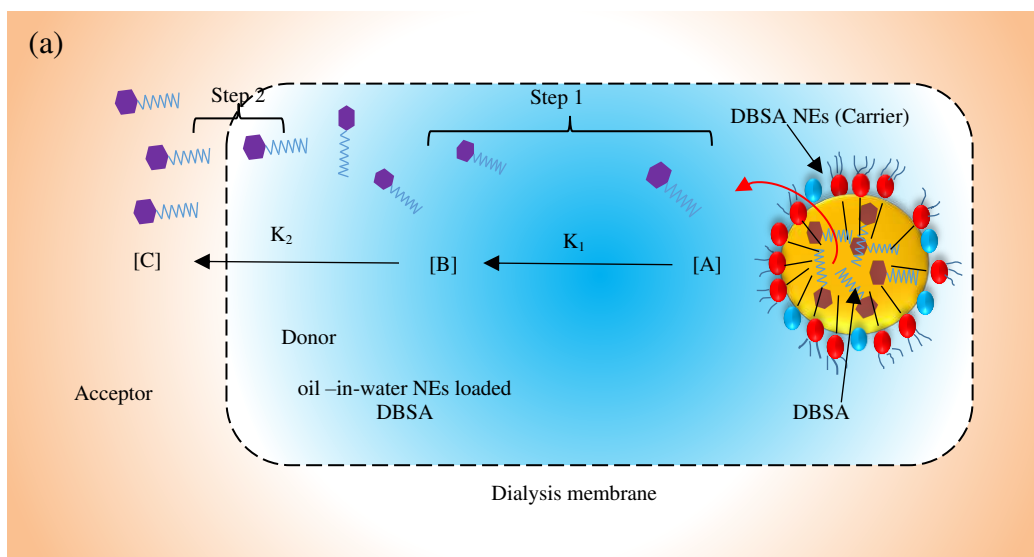


Figure 10: Release or transport profiles of DBSA through the dialysis membrane from (A) xylene and (B)DBSA NEs.

Table 3: Influence of DBSA concentration and droplet sizes on the cumulative of DBSA released % through the dialysis membrane after 24 hr.

DBSA concentration (vol. %)	DBSA NEs				DBSA in xylene
	d (nm)	PDI	Zeta potential (mV)	DBSA released (%)	DBSA transported (%)
1.0	21	0.19	-33	99.0	13.7
2.0	93	0.21	-34	87.6	12.25
3.0	135	0.36	-33	72.2	11.65
4.0	274	0.44	-30	67.2	11.15

In the dialysis membrane testing, there are two kinetics steps involved in the total inhibitor release: 1) the inhibitor is released from the NEs to the medium inside the donor ( $k_1$ , see Figure 11a & b), and 2) the released inhibitor inside the donor diffuses across the membrane to the acceptor due to concentration gradient and its high affinity for oil phase in the acceptor ( $k_2$ , see Figure 11a & b). On the other hand, a poor membrane permeation of DBSA from xylene in comparison to DBSA NEs clearly indicated a higher intermolecular interaction between DBSA and xylene in the donor media; this may result in aggregation and formation of self-assembly in the donor compartment ( $k_3$  and  $-k_3$ , see Figure 11b). This could explain why the accumulative DBSA transported through membrane is small in the case of using DBSA in xylene.



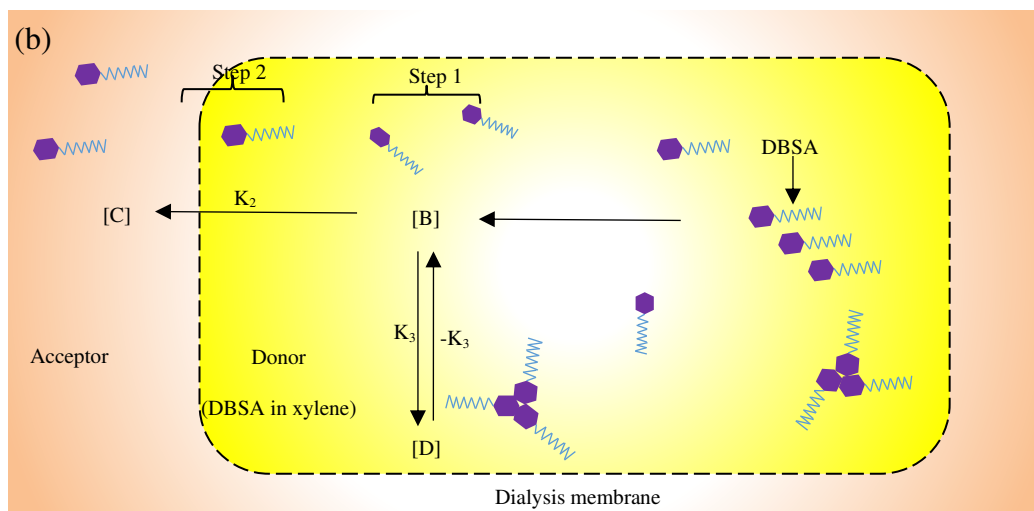


Figure 11: Schematic of the kinetic processes of inhibitor transport and release through the dialysis membrane for (a) DBSA NEs and (b) DBSA in xylene. [A] – DBSA concentration in the NEs, [B] – DBSA concentration in the in the donor, [C] – inhibitor concentration in the receptor, and [D] – DBSA concentration in the donor.  $K_1$  is the diffusion rate constants of inhibitor inside the dialysis bag,  $K_2$  and  $-K_2$  are the diffusion rate constant of inhibitor through a dialysis membrane to receptor, and,  $K_3$  is the diffusion rate constant of inhibitor at formation aggregates in the donor.

It is essential to study the release kinetics for a better understanding the efficacy of NE to deliver and release DBSA. The selection of a suitable kinetic model for fitting the inhibitor release data helps determine the release characteristics. There are number of kinetic models, which describe the overall release of drug from the carrier [26-28]. The most common mathematical models used in this study to investigate the release of DBSA from NEs and DBSA transport from xylene through the dialysis membrane are presented in Table 4.

Table 4: The kinetic model parameters fitting to the DBSA release or transport results.

Models	Mathematical models	Parameters	DBSA in NEs	DBSA in xylene
Zero-order	$F = F_0 + K_0 \cdot t$	R <sup>2</sup> K <sub>0</sub>	0.98151 0.000627722	0.96981 0.0000949912
First order	$\ln(1 - F) = -K_1 \cdot t$	R <sup>2</sup> K <sub>1</sub>	0.61938 0.00251	0.97217 0.000102931
Higuchi	$F = F_0 + K_H \cdot t^{1/2}$	R <sup>2</sup> K <sub>H</sub>	0.98204 0.02585	0.97142 0.00389
Korsmeyer-Peppas	$F_t = F_0 + K_{HP} \cdot t^n$	R <sup>2</sup> K <sub>HP</sub> n	0.99805 0.00628 0.68991	0.96414 0.000768552 0.51113
Baker-Lonsdale	$3/2[1 - (1 - Ft)^{2/3}] - Ft = K_{BL}t$	R <sup>2</sup> K <sub>BL</sub>	0.72421 0.000328911	0.96702 0.000110438
Hixon-Crowell	$1 - (1 - F_t)^{1/3} - F_t = K_{HC}t$	R <sup>2</sup> K <sub>HC</sub>	0.88113 0.00045031	0.97146 0.0000333992
Square root of mass	$1 - (1 - F_t)^{1/2} - F_t = K_{SR}t$	R <sup>2</sup> K <sub>SR</sub>	0.95244 0.000534237	0.97107 0.000049432
Three seconds root of mass	$1 - (1 - F_t)^{2/3} = K_{TS}t$	R <sup>2</sup> K <sub>TS</sub>	0.98463 0.000582836	0.97067 0.0000650347

where:  $F_t$ – the amount of drug released in time  $t$ ,

$F_0$  : the initial amount of drug,

$K_0$ : zero order kinetic constant,

$K_1$  : first order kinetic constant,

$K_H$  : Higuchi kinetic constant,

$K_{HP}$ : Korsmeyer-Peppas release constant,

$K_{BL}$ : Baker-Lonsdale release constant,

$K_{HC}$ : Hixon- Crowell release constant,

$K_{SR}$  : Square root of mass release constant,

$K_{TS}$  : Three second root of mass release constant,

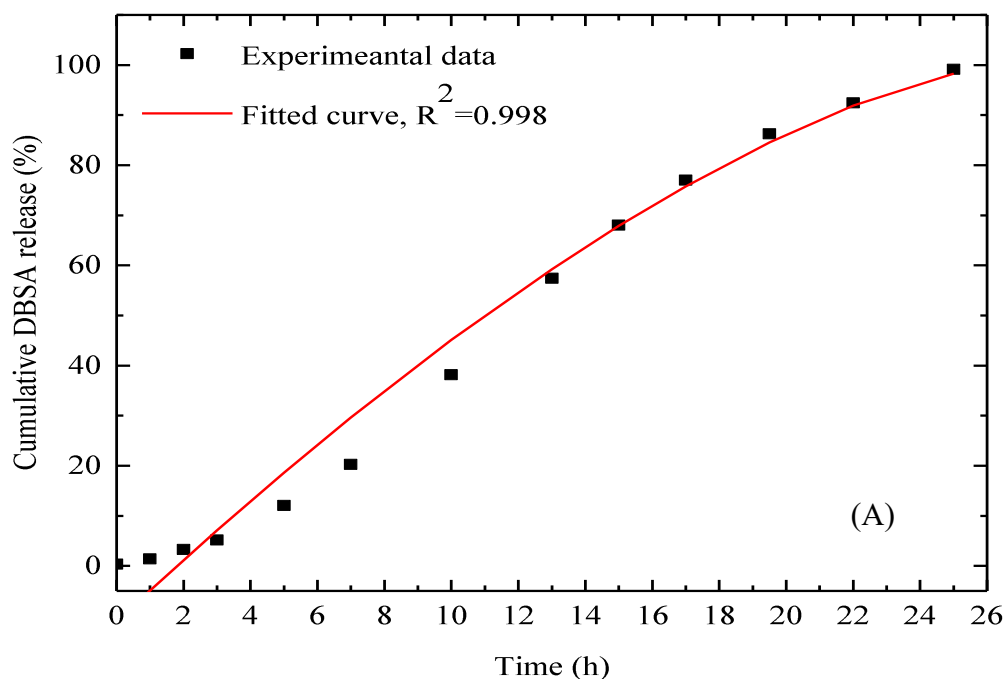
$n$ : diffusional release exponent,

$t$ : time.

It can be seen from the data in Table 4 that the best kinetic fit of DBSA release from NE was described by Korsmeyer-Peppas model, also confirmed by the coefficient of determination,  $R^2 = 0.99805$  (highest value). The parameter “ $n$ ” in the Korsmeyer-Peppas equation is related to the mechanism of release of the inhibitor, i.e. if the exponent  $n < 0.43$ , then the release mechanism is Fickian diffusion, if  $0.43 < n < 0.85$ , then it is non-Fickian or anomalous diffusion and an exponent value is 0.85 or greater is indicative of Case-II Transport or typical zero-order release [37,38]. In this case, DBSA NEs give a value of  $n$  of 0.68, so their release mechanism followed a non-Fickian or anomalous diffusion. This suggested there is a strong interaction among DBSA molecules and the NE's components, which confirms that the DBSA is released slowly, dependent on the inhibitor concentration in the NE. A slow release DBSA from NEs overtime can provide long-lasting stability and minimize the amount of inhibitor. Therefore, this result clearly highlights that DBSA NE systems can act as better inhibitor carrier for controlled release of DBSA with a prolonged release profile. This data is in accordance with a large number of recent drug release studies Rodríguez-Burneo et al. [39], Alvarado et al. [40], which showed that the Korsmeyer-Peppas model best describes a release process of drugs.

On the other hand, in the case of using DBSA in xylene, the DBSA transported profiles through the dialysis membrane could be best explained by first order or Higuchi models. Both regression lines are characterized by higher  $R^2$  values than initial ( $R^2 > 0.97$ ). This indicates an initial burst transport of DBSA from xylene; however, no significant cumulative transport efficacy is

achieved. This result is in agreement with those obtained by Miastkowska et al. [41], and Nanjwade et al. [42], who suggested that the release oil soluble drug from the oil phase could be best explained by Higuchi or first order. Figure 12 (a and b) shows the release profiles of 1 vol.% DBSA from NEs and fitted to the Korsmeyer-Peppas mode, and the transport profiles of 1 vol. % DBSA from xylene and fitted to the first order mode. All the kinetic models fitting to the DBSA release from NEs and xylene through the dialysis membrane are illustrated in S2 in the Supplementary Information.



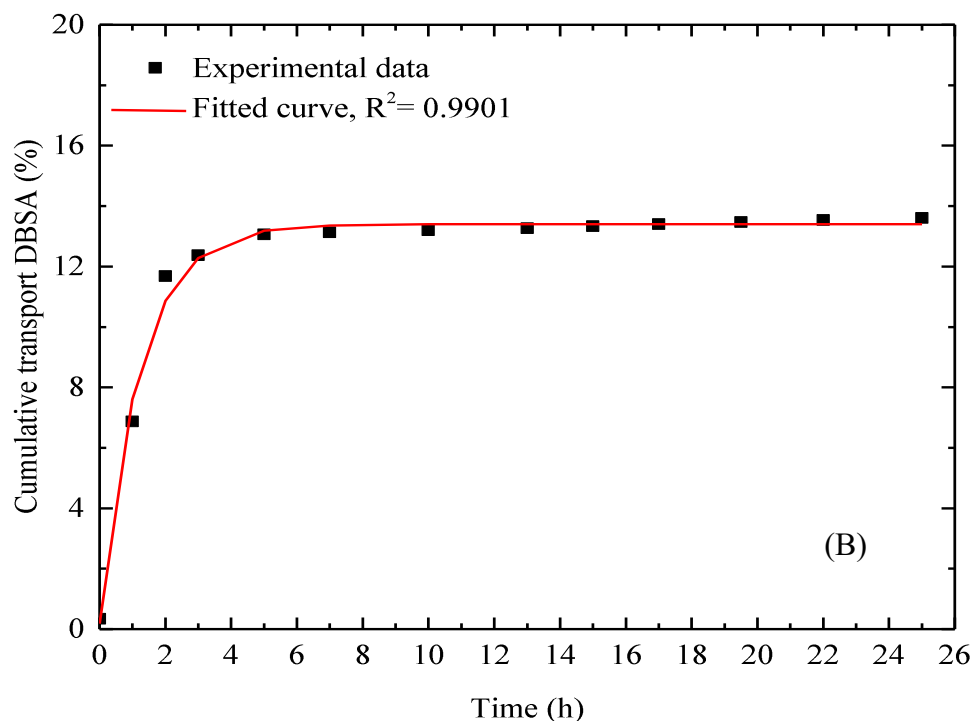


Figure 12: (A) The release profiles of 1 vol.% DBSA from NEs and fitted to the Korsmeyer-Peppas mode ( $n = 0.68$ ), and (B) The transport profiles of 1 vol.% DBSA from xylene and fitted to the first order mode.

### 3.4. Relationship between DBSA released from NEs in asphaltene solution and its release through membrane

The relationship between the Turbiscan technique data (% transmission, see Figure 5) and membrane dialysis method data (% cumulative of DBSA released, see Figure 10B) was correlated at the same time points (point-to-point) without any change in the time scale. The release profile of DBSA from NEs through membrane was confirmed by deconvolution to the Korsmeyer-Peppas model. The main objective to use this methodology (see Section 2.6) is to support our proposed mechanisms: the asphaltene stability with DBSA NEs and the kinetic steps

of inhibitor transport/release through the dialysis membrane, as discussed in Sections 3.2 and 3.3 respectively. This methodology can also be employed to establish release specifications and to support and/or validate the use of release methods. A good correlation is a tool for predicting asphaltene performance and stability based on kinetic release data of AI through membrane.

It is interesting to note that a second order polynomial correlation is found between % cumulative release obtained from the membrane dialysis method (X) and % transmission obtained from Turbiscan technique data (Y) with a correlation coefficient ( $R^2$ ) of 0.9315 (Figure 13). This may indicate a strong correlation between the two methods. It can also be observed that, up to 3h, light transmission can increase along the measuring cell because the settle down of some asphaltene clusters, and the corresponding cumulative release of DBSA was about 15 %, which can not affect asphaltene clusters. There is, however, after 4 h, the transmission dropped progressively when the release rate increases, confirming that small particles are formed, and therefore this is an indicator of keeping the asphaltenes well-solubilized in the solution, which is in perfect agreement with data obtained by particle size measurements. The good correlation among the measurements obtained by the different techniques indicates that this methodology is useful to quantify the time needed for the release to occur and to determine the minimum AI concentration that starts to interact with asphaltene. Furthermore, from the data in Figure 13, it has been able to provide a robust evidence for supporting the above proposed release mechanism (see Section 3.2). The proposed mechanism, based upon the release of DBSA and components from NEs and their influence on transmission within 24 h, suggests that the release kinetic can be occurred within three stages: 1) the first plateau corresponds to the adsorption of self-assembled asphaltene at the interface; 2) DBSA NEs adsorption at interface induced release of entrapped DBSA, and 3) the breakage of clusters into the bulk due to the release DBSA NEs components.

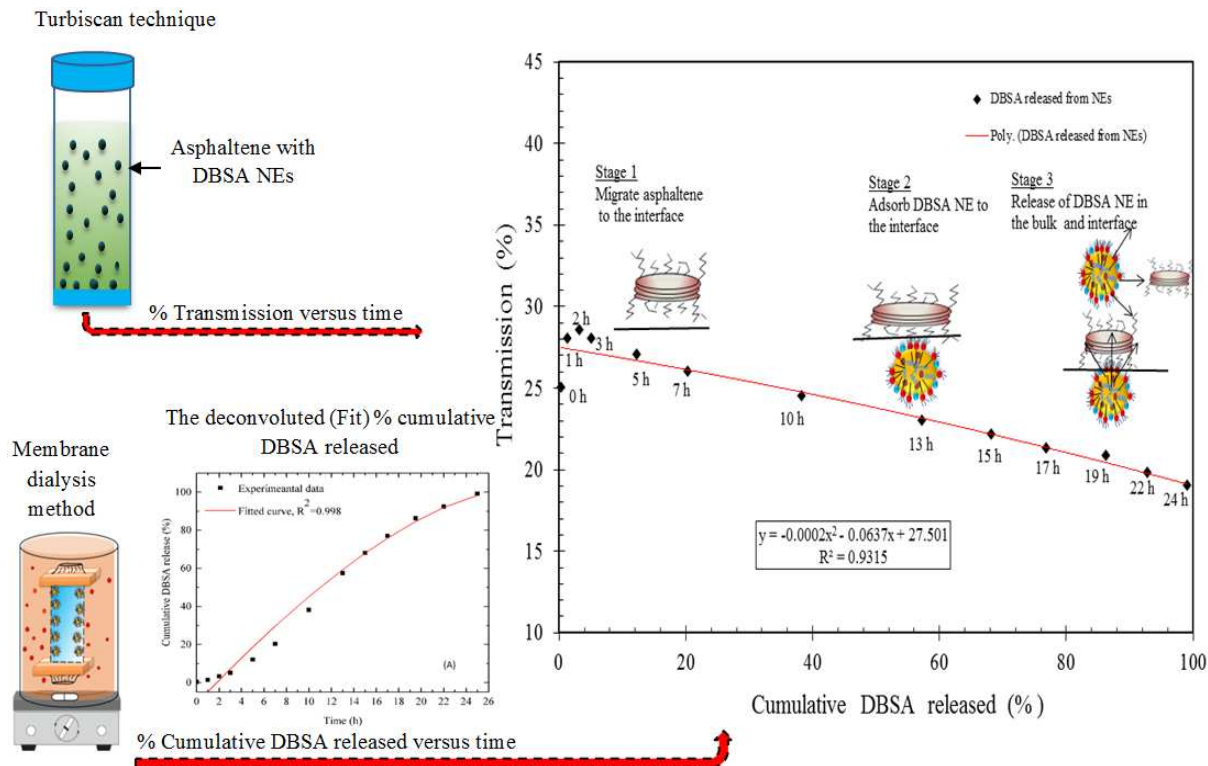


Figure 13: The relationship between the transmission and cumulative DBSA released. This plot presents schematic of a possible mechanism of DBSA NEs adsorption at interface induced release of entrapped DBSA. The first plateau corresponds to adsorption of self-assembled asphaltene at the interface. However, with time, the asphaltene undergo disassembly (break down clusters) into the bulk due to release DBSA NEs components, and the final transmission decreased corresponds to the increase the release rate.

#### 4. Conclusions

This is the first attempt to develop the concept of controlled delivery of asphaltene inhibitor by using NEs. Both *in situ* and kinetic release experiments confirmed the validity of the new concept:

- The DBSA and other components are progressively released from NE and interact with asphaltene molecules, increasing the stability of asphaltene.
- DBSA NEs can significantly increase the efficiency of asphaltene inhibition by 84.12 % after 24 h, showing its effectiveness with increasing release time.
- DBSA NEs are able to reduce asphaltenes from precipitate to spherical nanometric particles (5 to 30 nm), delaying the onset of asphaltene precipitation.
- The rate of DBSA released through the dialysis membrane increases as the droplet size decreases, which is attributed to the increase in the surface area of the NEs.
- The released amount of DBSA was much higher from NE (99 %) than from the xylene (13 %). The release profile of DBSA NEs follows that Korsmeyer-Peppas mode kinetic model.
- The strong correlation between % DBSA released and % transmission clearly indicated the possibility of predicting the release time and the minimum DBSA released amount based on the kinetic processes of inhibitor release through the dialysis membrane studies.

- There is a significant advantage in using NEs loaded DBSA to achieve prolonged asphaltene treatment with reduced amount of inhibitor, rather than directly mixing DBSA in xylene.
- It suggests that direct treatment of asphaltene with DBSA in both upstream and downstream should be avoided and there is not extended and efficient treatment effect.

Acknowledgement This work was supported by European Research Council Consolidator Grant (Grant number: 648375).

## References

- [1] Silva, F. B.; Guimarães, M. J. O. C.; Seidl, P. R.; Garcia, M. E. F. Extraction and characterization (compositional and thermal) of asphaltenes from Brazilian vacuum residues. *Braz J. Petrol Gas* **2013**, 7, 107–118.
- [2] Ancheyta, J.; Speight, J. Hydroprocessing of heavy oils and residua; Boca Raton: CRC Press: **2007**.
- [3] Leontaritis, K. J.; Mansoori, G. A. Asphaltene flocculation during oil production and processing: a thermodynamic colloidal model. In: SPE International Symposium on Oilfield Chemistry. San Antonio: SPE; **1987**.
- [4] Nghiem, L. X.; Coombe, D. A. Modeling Asphaltene Precipitation during primary depletion. In: Fourth Latin American and Caribbean Petroleum Engineering Conference. Trinidad & Tobago: SPE; **1996**.
- [5] Wang, J. X.; Buckley, J. S. A two-component solubility model of the onset of asphaltene flocculation in crude oils. *Energ Fuel* **2001**, 15, 1004–1012.
- [6] Alboudwarej, H.; Akbarzadeh, K.; Beck, J.; Svrcek, W. Y.; Yarranton H. W. Regular solution model for asphaltene precipitation from bitumens and solvents. *AIChE J.* **2003**, 49, 2948–2956.
- [7] Gonzalez, D. L.; Hirasaki, G. J.; Creek, J.; Chapman, W. G. Modeling of asphaltene precipitation due to changes in composition using the perturbed chain statistical associating fluid theory equation of state. *Energ Fuel* **2007**, 21, 1231–1242.
- [8] Balson, T.; Craddock, H. A.; Dunlop, J.; Frampton, H.; Payne, G.; Reid, P.; Oschmann, H. J. New methods for the selection of asphaltene inhibitors in the field. *Chem. Oil Industry VII*: **2002**, 254–263.
- [9] Gupta, D.; Szymczak, S.; Brown, M. Solid production chemicals added with the frac for scale, paraffin and asphaltene inhibition. In: SPE Hydraulic Fracturing Technology Conference. Society of Petroleum Engineers; **2009**.
- [10] Bouts, M. N.; Wiersma, R. J.; Muijs, H. M.; Samuel, A. J. An evaluation of new asphaltene inhibitors; Laboratory study and field testing. *Journal of Petroleum Technology* **1995**, 47(09), 782–787.
- [11] Goual, L.; Sedghi, M.; Wang, X.; Zhu, Z. Asphaltene aggregation and impact of alkylphenols. *Langmuir* **2014**, 30(19), 5394–5403.
- [12] Lifshitz, I. M.; Slyozov, V. V. The kinetics of precipitation from supersaturated solid solutions. *J. Phys. Chem. Solids* **1961**, 19(1–2), 35–50.
- [13] Souza, V. B.; Neto, J. S.; Spinelli, L. S.; Mansur, C. R. Application of oil/water nanoemulsions as a new alternative to demulsify crude oil. *Separation Science and Technology* **2013**, 48(8), 1159–1166.
- [14] Souza, V. B.; Mansur, C. R. Oil/Water nanoemulsions: Activity at the water–oil interface and evaluation on asphaltene aggregates. *Energ Fuel* **2015**, 29(12), 7855–7865.

- [15] Oliveira, P. F.; Farias, N. C.; Marques, A. M.; Fraga, A. K., Mansur, C. R. Development of nanoemulsions containing a polyoxide surfactant and asphaltene dispersant. *Fuel* **2016**, 181, 64–74.
- [16] Alhreez, M.; Wen, D. Controlled releases of asphaltene inhibitors by nanoemulsions. *Fuel* **2018**, 234, 538–548.
- [17] Cai, S.; Zhao, M.; Fang, Y.; Nishinari, K.; Phillips, G. O.; Jiang, F. Microencapsulation of *Lactobacillus acidophilus* CGMCC1.2686 via emulsification/internal gelation of alginate using Ca-EDTA and CaCO<sub>3</sub> as calcium sources. *Food Hydrocolloids* **2014**, 39, 295–300.
- [18] Costa, P.; Lobo, J. M. S. Modeling and comparison of dissolution profiles. *European Journal of Pharmaceutical Sciences* **2001**, 13(2), 123–133.
- [19] Dash, S.; Murthy, P. N.; Nath, L.; Chowdhury, P. Kinetic modeling on drug release from controlled drug delivery systems. *Acta Pol. Pharm.* **2010**, 67(3), 217–223.
- [20] Christopher, J.; Sarpal, A. S.; Kapur, G. S.; Krishna, A.; Tyagi, B. R.; Jain, M. C.; Jain, S. K.; Bhatnagar, A. K. Chemical structure of bitumen-derived asphaltene by nuclear magnetic resonance spectroscopy and X-ray diffractometry. *Fuel* **1996**, 75(8), 999–1008.
- [21] Yen, T. F.; Erdman, J. G.; Pollack, S. S. Investigation of the structure of petroleum asphaltene by X-ray diffraction. *Anal. Chem.* **1961**, 33(11), 1587–1594.
- [22] AlHumaidan, F. S.; Hauser, A.; Rana, M. S.; Lababidi, H. M.; Behbehani, M. Changes in asphaltene structure during thermal cracking of residual oils: XRD study. *Fuel* **2015**, 150, 558–564.
- [23] Aslan, S.; Firoozabadi, A. Effect of water on deposition, aggregate size, and viscosity of asphaltene. *Langmuir* **2014**, 30(13), 3658–3664.
- [24] Hoepfner, M. P.; Limsakoune, V.; Chuenmeechao, V.; Maqbool, T.; Fogler, H. S. A fundamental study of asphaltene deposition. *Energ Fuel* **2013**, 27(2), 725–735.
- [25] Juyal, P.; Ho, V.; Yen, A.; Allenson, S. J. Reversibility of asphaltene flocculation with chemicals. *Energ Fuel* **2012**, 26(5), 2631–2640.
- [26] de Almeida Borges, V.R., Simon, A., Sena, A.R.C., Cabral, L.M. and de Sousa, V.P., Nanoemulsion containing dapson for topical administration: a study of in vitro release and epidermal permeation. *International journal of nanomedicine* **2013**, 8, p.535.
- [27] Barradas, T.N., Senna, J.P., Cardoso, S.A., e Silva, K.G.D.H. and Mansur, C.R.E., Formulation characterization and in vitro drug release of hydrogel-thickened nanoemulsions for topical delivery of 8-methoxypsoralen. *Materials Science and Engineering* **2018**, 92, pp.245-253.
- [28] Nothnagel, L. and Wacker, M.G., How to measure release from nanosized carriers?. *European Journal of Pharmaceutical Sciences*. **2018**
- [29] Rodrigues, M. R.; Lanzarini, C. M.; Ricci-Junior, E. Preparation, in vitro characterization and in vivo release of naproxen loaded in poly-caprolactone nanoparticles. *Pharm. Dev. Technol.* **2011**, 16, 12–21.
- [30] Pereira, J. C.; Delgado-Linares, J.; Briones, A.; Guevara, M.; Scorzza, C.; Salager, J. L. The effect of solvent nature and dispersant performance on asphaltene precipitation from diluted solutions of instable crude oil. *Petroleum Science and Technology* **2011**, 29(23), 2432–2440.

[31] Colomer, M. T.; Guzman, J.; Moreno, R. Determination of peptization time of particulate sols using optical techniques: Titania as a case study. *Chemistry of Materials* **2008**, 20(12), 4161–4165.

[32] Alhreez, M.; Wen, D.; Ali, L. A novel inhibitor for controlling Iraqi asphaltene problems. International Conference on Environmental Impacts of the Oil and Gas Industries: Kurdistan Region of Iraq as a Case Study (EIOGI). Iraq; **2017**, 37–41.

[33] Mansur, C. R.; de Melo, A. R.; Lucas, E. F. Determination of asphaltene particle size: influence of flocculant, additive, and temperature. *Energ Fuel* **2012**, 26(8), 4988–4994.

[34] Hoepfner, M. P.; Vilas Bôas Fávero, C.; Haji-Akbari, N.; Fogler, H. S. The fractal aggregation of asphaltenes. *Langmuir* **2013**, 29(28), 8799–8808.

[35] Sjöblom, J.; Aske, N.; Auflem, I. H.; Brandal, Ø.; Havre, T. E.; Sæther, Ø.; Westvik, A.; Johnsen, E. E.; Kallevik, H. Our current understanding of water-in-crude oil emulsions: Recent characterization techniques and high pressure performance. *Advances in Colloid and Interface Science* **2003**, 100, 399–473.

[36] Tarafder, S., Nansen, K. and Bose, S., Lovastatin release from polycaprolactone coated  $\beta$ -tricalcium phosphate: Effects of pH, concentration and drug–polymer interactions. *Materials Science and Engineering* **2013**.: C, 33(6), pp.3121-3128.

[37] Peppas, N.A. Commentary on an exponential model for the analysis of drug delivery: Original research article: a simple equation for description of solute release: I II. Fickian and non-Fickian release from non-swellable devices in the form of slabs, spheres, cylinders or discs, 1987. *Journal of Controlled Release* **2014**, 190, 31–32.

[38] Elosaily, G. H. Formulation and in-vitro evaluation of nystatin nanoemulsion-based gel for topical delivery. *J. Am. Sci.* **2012**, 8(12), 541–548.

[39] Rodríguez-Burneo, N.; Busquets, M. A.; Estelrich, J. Magnetic nanoemulsions: Comparison between nanoemulsions formed by ultrasonication and by spontaneous emulsification. *Nanomaterials* **2017**, 7(7), 190.

[40] Alvarado, H. L.; Abrego, G.; Souto, E. B.; Garduño-Ramirez, M. L.; Clares, B.; García, M. L.; Calpena, A. C. Nanoemulsions for dermal controlled release of oleanolic and ursolic acids: in vitro, ex vivo and in vivo characterization. *Colloids and Surfaces B: Biointerfaces* **2015**, 130, 40–47.

[41] Miastkowska, M.; Sikora, E.; Ogonowski, J.; Zielina, M.; Łudzik, A. The kinetic study of isotretinoin release from nanoemulsion. *Colloids and Surfaces A: Physicochemical and Engineering Aspects* **2016**, 510, 63–68.

[42] Nanjwade, B. K.; Varia, P. J.; Kadam, V. T.; Srichana, T.; Kamble, M. S. Development and evaluation of nanoemulsion of repaglinide. *Nanotechnol. Nanomed.* **2013**, 1(2), 1–8.

